Available online at www.sciencedirect.com
SCIENCE DIRECT®
International Journal of Mass Spectrometry 234 (2004) 161–169
International Journal of Mass Spectrometry
www.elsevier.com/locate/ijms

The influence of spontaneous m/z-changes on the ion motion in an ion cyclotron resonance trap

Alexander Herlert, Lutz Schweikhard*

Institut für Physik, Ernst-Moritz-Arndt-Universität Greifswald, D-17487 Greifswald, Germany

Received 26 November 2003; accepted 11 February 2004

Dedicated to A.G. Marshall on the occasion of his 60th birthday.

Available online 17 April 2004

Abstract

The influence of mass-over-charge ratio (m/z) changing reactions on the motion of stored ions in a Penning trap (ion cyclotron resonance cell) is investigated. For all three motional modes, the cyclotron, the magnetron and the axial (trapping) motion, the influence of the m/z change on the amplitude is discussed. In cases of spontaneous m/z increase, as for electron loss from a polyanionic particle, the extension of the radial ion motion is increased and thus the ions may be lost from the trap. As an example, measurements on the electron emission from doubly charged cluster anions are discussed.

Keywords: Penning trap; Ion motion; Multiply-charged ions; Electron emission; Ion loss

1. Introduction

Ion cyclotron resonance mass spectrometry (ICR MS) has a long and successful history [1,2]. After initial experiments on ion molecular reactions with drift cells [3,4] a major milestone was the introduction of the trapped ion cell [5] which led to a partial merger of technical developments in the more chemistry and in the more physics related research. In the latter the ICR cells are usually referred to as Penning traps and are extensively used for mass spectrometric and laser spectroscopic experiments of highest accuracy [6–8]. For analytical chemistry the next major step was the introduction of Fourier transform ICR mass spectrometry (FT-ICR MS) [9] which makes use of fast Fourier transform methods [10,11] and thus gives an immediate access "in one shot" to the whole spectrum of stored ions from the smallest to the very big masses [12–14]. Further experimental progress followed in the form of the capturing of externally created ions [15–17]. This meant that sources which need an easy access or which are incompatible with the ultra high vacuum requirements of the ICR trap could produce the ions outside of the region of the trap's high magnetic field. The ions are transferred and injected into the trap where they are captured in flight. Thus, FT-ICR MS was well-prepared when MALDI [18,19] and electrospray [20] took the stage of ion production for bio-molecular mass spectrometry. The latter also at least partly removed a disadvantage of FT-ICR MS (as compared to the rival technique of time-of-flight mass spectrometry): the limited mass range for the storage of ions in an ICR (Penning) trap, due to the electric repulsion of the ions from the trap's center in the radial direction. This is often referred to as a "critical mass" limit, while in fact it should rather be called the critical m/z limit, where m stands for the mass and z for the charge state of the ions. Since electrospray allows to put many charges onto the ions (mostly by multiple protonation), large biomolecules with high masses are thus accessible to FT-ICR MS.

Similarly, high-mass atomic clusters may be stored in a Penning trap. Even for $z = 1$, gold clusters made up of 145 atoms, Au_{145}^{1-}, i.e. with a mass-over-charge ratio of almost $m/z = 30{,}000$ have been trapped [21]. We note in passing, that in contrast to other ion trapping devices, the m/z range for simultaneous trapping in Penning traps is enor-

* Corresponding author. Tel.: +49-3834-86-4750; fax: +49-3834-86-4701.
E-mail address: lutz.schweikhard@physik.uni-greifswald.de (L. Schweikhard).

1387-3806/$ – see front matter © 2004 Elsevier B.V. All rights reserved.
doi:10.1016/j.ijms.2004.02.017

mous: Since there is no lower mass limit electrons and heavy clusters can be stored at the same time and in these kinds of recent experiments the m/z range has exceeded seven orders of magnitude [22].

In this contribution the influence of a spontaneous change in the mass-over-charge ratio, m/z, on the motion of an ion stored in a Penning trap is investigated. As discussed in detail, the ion trajectory can change significantly. In particular when the ion has been prepared in a pure cyclotron or magnetron motion prior to the m/z-change it will in general acquire a mixed motion after the reaction. This can lead to a significant increase in the extension of the orbit from the trap's axis and can thus result in severe ion loss. This loss of signal intensity is solely based on the ion-trajectory change by a unimolecular reaction, i.e. not due to any "external" influence as rf excitations, trap imperfections or momentum-transferring collisions. A short report of the effect on the radial ion motion in the case of electron loss from a dianion and some experimental illustration by collision-induced activation of dianionic gold clusters has already been given in [23,24]. In the following this discussion is refined and extended.

2. Description of trapped ion motion

2.1. Overview of ion motion in the Penning trap

The ideal Penning trap and its properties have been discussed extensively by Brown and Gabrielse [25]. In Fig. 1a one particular geometry of a Penning trap with hyperbolically shaped electrodes is shown. The trap dimension is characterized by $d_0 = \sqrt{r_0^2 + 2z_0^2}/2$ where $2r_0$ is the diameter of the ring electrode and $2z_0$ is the distance of the endcap electrodes. For ion storage a static potential U_0 is applied between the ring and the endcap electrodes together with a homogeneous magnetic field $\vec{B}$ along the z-axis. Thus, the motion of an ion with mass m and charge $q = ze$ in a Penning trap is a linear superposition of three independent modes: A harmonic oscillation along the magnetic field lines (z-direction) at an angular frequency of:

$$\omega_z = \sqrt{\frac{qU_0}{md_0^2}} \tag{1}$$

and two radial circular modes, in the xy-plane perpendicular to the magnetic field at frequencies:

$$\omega_\pm = \frac{\omega_c}{2} \pm \sqrt{\frac{\omega_c^2}{4} - \frac{\omega_z^2}{2}} \tag{2}$$

where ω_+ is called reduced cyclotron frequency and ω_- magnetron frequency. $\omega_c = qB/m$ is the frequency of the free cyclotron motion in the magnetic field B.

Thus there is an upper mass limit, sometimes also called critical mass for a given set of trapping conditions, i.e. B,

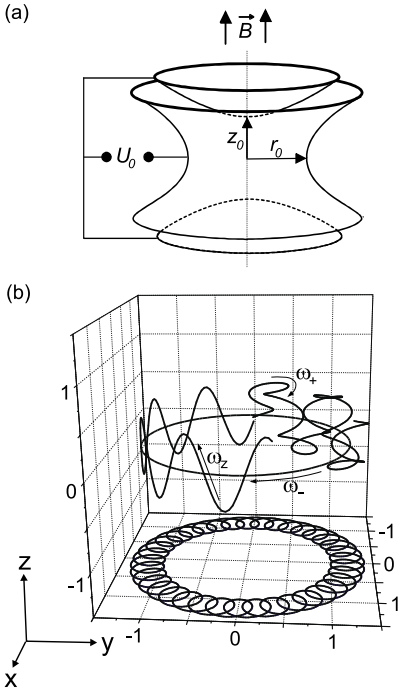

Fig. 1. (a) Penning trap electrodes with the indication of the radial and axial dimensions r_0 and z_0. (b) Trajectory of a gold cluster ion Au_{20}^{1-} for experimental parameters $\pi_{trap} = 0.1$, $r_+ = 0.2$, $r_- = 1.2$, and $z_{max} = 0.4$, where the three motional modes are superposed consecutively for clarity. The lower trajectory shows the projection of the radial plane.

U_0, and the trap dimension d_0 (for cubic, cylindric and other geometries a respective dimensionless numerical factor is introduced for the determination of d_0 [26]). More precisely, there is a limit as to which ions (ions of what mass-to-charge ratio) have a stable trajectory, i.e. a path which forever keeps within a finite distance from the trap's center:

$$\frac{m}{q} < \frac{B^2 d_0^2}{2U_0} = \left(\frac{m}{q}\right)_{crit} \tag{3}$$

Fig. 1b gives an impression of the combination of the motional modes. The particular amplitudes and phases depend on the "initial conditions". For later use we reformulate the expressions for the characteristic frequencies in terms of the trapping parameter [21]:

$$\pi_{trap} = 2\frac{\omega_z^2}{\omega_c^2} = \frac{m}{q}\frac{2U_0}{B^2 d_0^2} = \frac{m/q}{(m/q)_{crit}} \tag{4}$$

which has to fulfill the condition $0 < \pi_{trap} < 1$ for stable trajectories:

$$\omega_z = \omega_c\sqrt{\frac{\pi_{trap}}{2}} \tag{5}$$

$$\omega_\pm = \frac{\omega_c}{2}(1 \pm \sqrt{1 - \pi_{trap}}) \tag{6}$$

Fig. 2 shows these frequencies in units of the cyclotron frequency ω_c as a function of the trapping parameter. An ion thus follows a path described by:

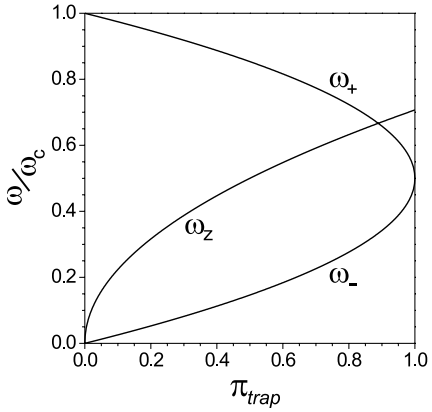

Fig. 2. Frequencies (in units of the cyclotron frequency ω_c) of the cyclotron motion (ω_+), magnetron motion (ω_-) and axial motion (ω_z) as a function of the trapping parameter π_{trap}.

$$x(t) = r_+ \sin(\omega_+ t + \phi_+) + r_- \sin(\omega_- t + \phi_-) \quad (7)$$

$$y(t) = r_+ \cos(\omega_+ t + \phi_+) + r_- \cos(\omega_- t + \phi_-) \quad (8)$$

$$z(t) = z_{max} \sin(\omega_z t + \phi_z) \quad (9)$$

where for simplicity the phase terms of the radial modes can be set to zero ($\phi_+ = \phi_- = 0$) as allowed by a respective choice of the orientation of the coordinate system.

2.2. Sudden change of m/z

In the following a sudden change of the mass-over-charge ration of the stored ion from m/z to M/Z is considered with respect to the influence on its trapping conditions. In general, the ion will follow a new path with new motional amplitudes, frequencies and phases:

$$X(t) = R_+ \sin(\Omega_+ t + \Phi_+) + R_- \sin(\Omega_- t + \Phi_-) \quad (10)$$

$$Y(t) = R_+ \cos(\Omega_+ t + \Phi_+) + R_- \cos(\Omega_- t + \Phi_-) \quad (11)$$

$$Z(t) = Z_{max} \sin(\Omega_z t + \Phi_z) \quad (12)$$

The ratios between the free cyclotron frequencies and the trapping parameters before and after the change in m/z are given by:

$$\frac{\Omega_c}{\omega_c} = \frac{m}{q}\frac{Q}{M} = \frac{m}{z}\frac{Z}{M} \quad (13)$$

$$\frac{\Pi_{trap}}{\pi_{trap}} = \frac{M}{Q}\frac{q}{m} = \frac{M}{Z}\frac{z}{m} \quad (14)$$

and thus

$$\frac{\Omega_c}{\omega_c} = \frac{\pi_{trap}}{\Pi_{trap}} \quad (15)$$

where capital letters are used to indicate variables after the reaction. For the characteristic frequencies the result of the m/z change is:

$$\Omega_z = \Omega_c \sqrt{\frac{\Pi_{trap}}{2}} = \omega_z \sqrt{\frac{m}{z}\frac{Z}{M}} \quad (16)$$

$$\Omega_\pm = \frac{\Omega_c}{2}(1 \pm \sqrt{1 - \Pi_{trap}}) = \frac{m}{z}\frac{Z}{M}\frac{\omega_c}{2}\left(1 \pm \sqrt{1 - \frac{M}{Z}\frac{z}{m}\pi_{trap}}\right) \quad (17)$$

A sudden change in the trapping conditions results in an immediate change in the amplitudes of the motional modes. Note, that throughout this contribution additional effects on the ion motion due to a kinetic energy release or a Coulomb interaction between the products are neglected. We only consider the effect of a sudden change in mass and/or charge state.

2.3. Change of radial motion

While the axial mode can be treated separately, an m/z-changing process leads to a redistribution of the amplitudes of the two radial motional modes. In the following two cases are considered in detail: The ion initially performs either a pure cyclotron or a pure magnetron motion, i.e. the amplitudes of the magnetron, respectively cyclotron, motion are negligible. Under these assumptions the initial phases ϕ_+ and ϕ_- can be set to zero without any loss of generality. (The general case is a straightforward extension, although it is more tedious and leads to complicated expressions since the relative phase of the modes at the time of the m/z-changing process has to be taken into account.)

2.3.1. Pure cyclotron motion

With $r_- = 0$ the ion trajectory before the reaction is given by:

$$x(t) = r_+ \sin(\omega_+ t) \quad (18)$$

$$y(t) = r_+ \cos(\omega_+ t) \quad (19)$$

i.e. the velocity components are

$$\dot{x}(t) = r_+ \omega_+ \cos(\omega_+ t) \quad (20)$$

$$\dot{y}(t) = -r_+ \omega_+ \sin(\omega_+ t) \quad (21)$$

The time of the change from m/z to M/Z may be chosen to be $t = 0$. Thus

$$x(t=0) = 0 = R_+ \sin(\Phi_+) + R_- \sin(\Phi_-) \quad (22)$$

$$y(t=0) = r_+ = R_+ \cos(\Phi_+) + R_- \cos(\Phi_-) \quad (23)$$

and

$$\dot{x}(t=0) = r_+ \omega_+ = R_+ \Omega_+ \cos(\Phi_+) + R_- \Omega_- \cos(\Phi_-) \quad (24)$$

$$\dot{y}(t=0) = 0 = -R_+ \Omega_+ \sin(\Phi_+) - R_- \Omega_- \sin(\Phi_-) \quad (25)$$

are the relations that determine the amplitudes and phases after the reaction. Before the respective equations are presented, it is useful to get an intuitive understanding of the

process. If the ion loses some mass, its reduced cyclotron frequency is increased: $\Omega_+ > \omega_+$. Since the velocity (which is mainly determined by the cyclotron motion) has not changed, $\Omega_+ R_+ \simeq \omega_+ r_+$, the cyclotron radii have to compensate the frequencies and thus $R_+ < r_+$. However, the position also has not changed instantaneously and thus the change of the cyclotron radius has to be compensated by the introduction of a finite magneton radius.

The full solution is given by the new amplitudes:

$$R_+ = \frac{\omega_+ - \Omega_-}{\Omega_+ - \Omega_-} r_+ \tag{26}$$

$$R_- = \frac{\omega_+ - \Omega_+}{\Omega_+ - \Omega_-} r_+ \tag{27}$$

and initial phases $\Phi_+ = 0$ and $\Phi_- = \pi$. In the case of $M/Z > m/z$ the sum of both amplitudes is given by:

$$R_+ + R_- = \frac{2\omega_+ - \Omega_c}{\Omega_+ - \Omega_-} r_+ \tag{28}$$

It is a measure of how far from the trap axis the ion motion extends. For $M/Z \leq m/z$ this maximum distance from the trap's axis is not changed by the reaction, i.e. it is given by the original cyclotron radius: $R_+ + R_- = r_+$. For $M/Z > m/z$, however, the trajectories' extensions are increased. In terms of the trapping parameter $\pi_{\text{trap}} \leq \Pi_{\text{trap}}$ the sum of the amplitudes can be rewritten as:

$$\frac{R_+ + R_-}{r_+} = \frac{(\Pi_{\text{trap}}/\pi_{\text{trap}})(1 + \sqrt{1 - \pi_{\text{trap}}}) - 1}{\sqrt{1 - \Pi_{\text{trap}}}} \tag{29}$$

This result is summarized in Fig. 3a, where the increase of the ion motion $(R_+ + R_-)/r_+$ is shown as a function of the initial and the final trapping parameter π_{trap} and Π_{trap}, respectively. Only in the case $\Pi_{\text{trap}} > \pi_{\text{trap}}$ the change of m/z may lead to an increase, largest for $\pi_{\text{trap}} < 0.2$ and $\Pi_{\text{trap}} > 0.8$. For further illustration the extension of the new ion motion $(R_+ + R_-)/r_+$ is plotted in Fig. 3b as a function of the initial trapping parameter π_{trap} and the ratio of the mass-over-charge ratios $f = (M/Z)/(m/z)$. The upper plateau shows the region of instable trajectories after the change of m/z. For $f \leq 1$ no change occurs while for $f > 1$ and depending on π_{trap}, i.e. the particular initial experimental parameters, the same ratio f may or may not lead to a loss of the product ion, when the new extension of the ion motion relative to the ring electrode dimension is taken into account.

As an example, which will be of relevance in the experimental section below, consider the case of electron emission from a doubly charged cluster anion of n atoms, Au_n^{2-}. In Fig. 4a the change of the radial frequencies is plotted as a function of the trapping parameter. It is obvious, that only for $\pi_{\text{trap}} < 0.5$ stable trajectories may be acquired for the product monoanion. The extension of the new trajectory depends on π_{trap}. For $\pi_{\text{trap}} = 0.1$ the resulting change in the ion motion is shown in Fig. 4b. The pure cyclotron motion of the dianion (solid line) is transformed into a new ion motion of the monoanion with $R_+ \simeq 2.1 r_+$ and $R_- \simeq 1.1 r_+$ and thus an extension of $R_+ + R_- \simeq 3.2 r_+$.

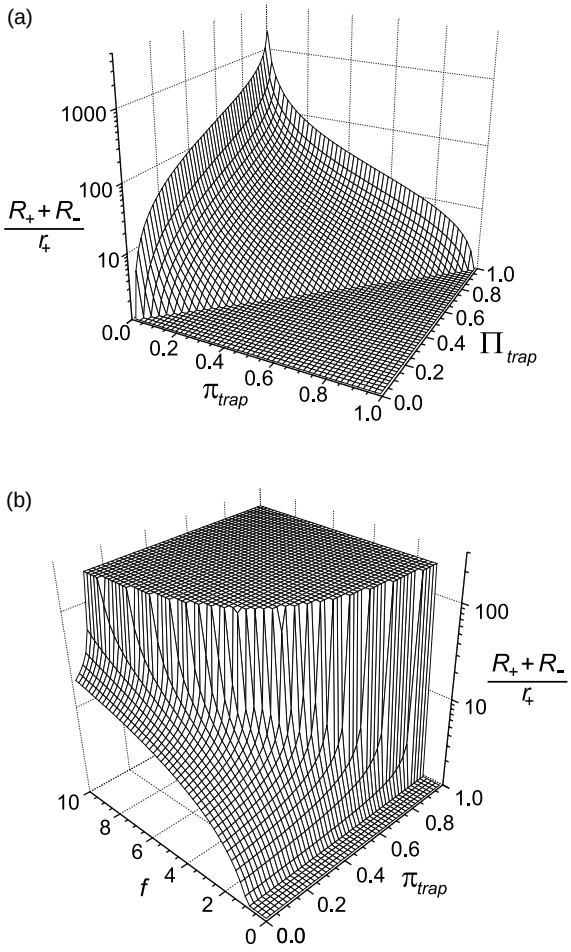

Fig. 3. (a) Relative increase $(R_+ + R_-)/r_+$ of the ion motion extension as a function of the trapping parameters π_{trap} and Π_{trap} before and after the change of m/z, respectively. (b) Relative increase of the ion motion extension as a function of the trapping parameter π_{trap} and the ratio $f = (M/Z)/(m/z)$.

Another example is the fission of the cation Au_{12}^{2+} into the products Au_9^+ and Au_3^+ as observed earlier in the Cluster Trap [27,28]. Fig. 5 shows how the two product clusters Au_9^+ and Au_3^+ continue to move in the xy-plane of the trap ($\pi_{\text{trap}} = 0.2$). In the case of Au_3^+ the new cyclotron radius is $R_+ \simeq 0.47 r_+$ and the new magnetron radius $R_- \simeq -0.53 r_+$ (the minus sign indicates an initial phase of π of the magnetron motion) which in total does not change the ion motion extension. This behavior is expected since $M/Z < m/z$. However, for Au_9^+ the new radii are $R_+ \simeq 1.6 r_+$ and $R_- \simeq 0.6 r_+$, which leads to an increase of $R_+ + R_- \simeq 2.2 r_+$ and possibly to a loss of the product ion.

2.3.2. Pure magnetron motion

Compared to the cyclotron motion a m/z-change during a pure magnetron motion is not very spectacular. In analogy to the last section, at time $t = 0$ the initial motion:

$$x(t) = r_- \sin(\omega_- t) \tag{30}$$

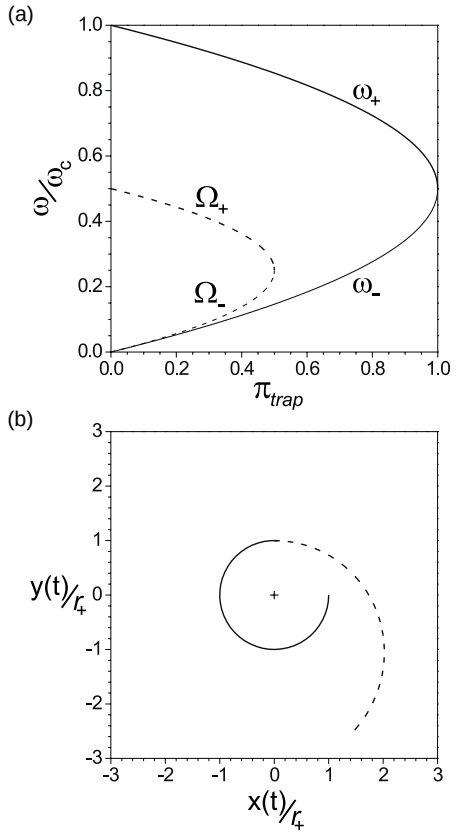

Fig. 4. (a) Frequencies of the cyclotron and magnetron motion of Au_n^{2-} before (solid line) and of Au_n^{1-} after the emission of an electron (dashed line). (b) Trajectory of a cluster ion Au_n^{2-} before (solid line) and of Au_n^{1-} after loss of one surplus electron (dashed line) for a trapping parameter $\pi_{\mathrm{trap}} = 0.1$. The time intervals before and after the decay process are equal.

$$y(t) = r_- \cos(\omega_- t) \tag{31}$$

with velocity components

$$\dot{x}(t) = r_- \omega_- \cos(\omega_- t) \tag{32}$$

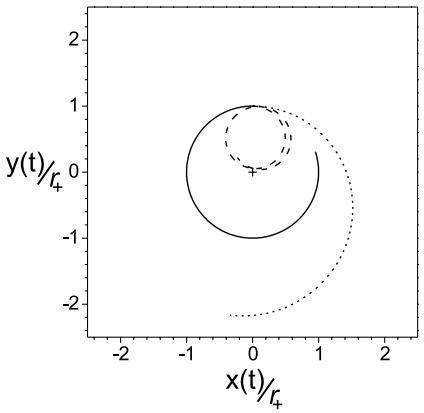

Fig. 5. Trajectories of Au_{12}^{2+} (solid line), Au_9^{1+} (dotted line), and Au_3^{1+} (dashed line) before and after asymmetric fission for a trapping parameter $\pi_{\mathrm{trap}} = 0.2$. The time intervals before and after the decay process are equal.

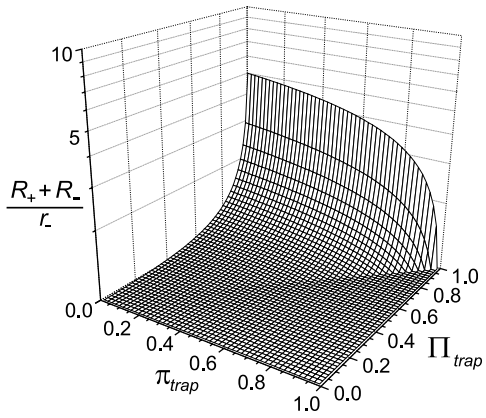

Fig. 6. Relative increase of the ion motion extension as a function of the trapping parameters π_{trap} and Π_{trap} before and after the change of m/z, respectively. The initial ion motion is purely a magnetron motion.

$$\dot{y}(t) = -r_- \omega_- \sin(\omega_- t) \tag{33}$$

is converted to a combined motion as described by Eqs. (22)–(25) where r_+ and $r_+\omega_+$ are to be replaced by r_- and $r_-\omega_-$, respectively. Thus the amplitudes after m/z conversion are given by:

$$R_+ = \frac{\Omega_- - \omega_-}{\Omega_+ - \Omega_-} r_- \tag{34}$$

$$R_- = \frac{\Omega_+ - \omega_-}{\Omega_+ - \Omega_-} r_- \tag{35}$$

in analogy to Eqs. (26) and (27) with phases $\Phi_+ = \pi$ and $\Phi_- = 0$. Obviously, in most cases of general interest, i.e. for $\omega_- \ll \Omega_+$ and $\Omega_- \ll \Omega_+$, the ion continues on its earlier trajectory with almost identical magnetron amplitude and a negligible new cyclotron component.

Again, the sum of both amplitudes is a measure of the extension of the ion motion: For $M/Z \leq m/z$ it is given by the original magnetron radius: $R_+ + R_- = r_-$ and for $M/Z > m/z$ the trajectories are increased:

$$R_+ + R_- = \frac{\Omega_c - 2\omega_-}{\Omega_+ - \Omega_-} r_- \tag{36}$$

In terms of the trapping parameter $\pi_{\mathrm{trap}} \leq \Pi_{\mathrm{trap}}$ the sum of the amplitudes can be rewritten as:

$$\frac{R_+ + R_-}{r_-} = \frac{1 - (\Pi_{\mathrm{trap}}/\pi_{\mathrm{trap}})(1 - \sqrt{1 - \pi_{\mathrm{trap}}})}{\sqrt{1 - \Pi_{\mathrm{trap}}}} \tag{37}$$

In Fig. 6 the extension of the ion motion after the change of m/z is plotted as a function of the trapping parameters before and after the reaction, π_{trap} and Π_{trap}, respectively. Only in case of values Π_{trap} close to one, a significant increase of the radii is observed, which is, however, several orders of magnitude smaller than in the case of a pure cyclotron motion.

2.4. Change of axial motion

In contrast to a pure cyclotron or a pure magnetron motion the phase angle $(\Omega_z t + \Phi_z)$ of the axial oscillation in the moment of m/z conversion has to be considered. Since the phase angle has been introduced explicitly above, the time of m/z-change can be chosen to be $t = 0$. Thus, from the spatial position at that time it can be followed:

$$z(t=0) = z_{\max} \sin(\phi_z) = Z_{\max} \sin(\Phi_z) \tag{38}$$

and from the velocity in the axial direction

$$\dot{z}(t=0) = z_{\max}\omega_z \cos(\phi_z) = Z_{\max}\Omega_z \cos(\Phi_z) \tag{39}$$

These two relations lead to the amplitude and phase after m/z conversion:

$$Z_{\max} = z_{\max}\sqrt{\frac{M}{Z}\frac{z}{m}\cos^2(\phi_z) + \sin^2(\phi_z)} \tag{40}$$

$$\Phi_z = \begin{cases} \arcsin\left(\dfrac{z_{\max}}{Z_{\max}}\sin(\phi_z)\right) & \text{for } -\dfrac{\pi}{2} \le \phi_z < \dfrac{\pi}{2} \\ \pi - \arcsin\left(\dfrac{z_{\max}}{Z_{\max}}\sin(\phi_z)\right) & \text{for } \dfrac{\pi}{2} \le \phi_z < \dfrac{3}{2}\pi \end{cases} \tag{41}$$

For an increase in m/z, i.e. $M/Z > m/z$, the amplitude will in general increase; for $M/Z < m/z$ it will decrease.

As an example, the fission of a doubly charged gold cluster cation Au_{12}^{2+} [27,28] is studied. In Fig. 7a the axial frequency ω_z of the precursor cluster Au_{12}^{2+} and its products Au_3^{1+} and Au_9^{1+} is plotted as a function of the trapping parameter. In accordance with Eq. (16), the frequency increases if $M/Z < m/z$ and decreases if $M/Z > m/z$. For a phase $\phi_z = 0$ the axial part of the ion motion follows the path shown in Fig. 7b, where the fission process takes place at $t = 0$.

In general, the new axial amplitude is a function of the phase angle in the instant of m/z-change as plotted in Fig. 7c for the cases $(M/Z)/(m/z) = 9/6 = 3/2$ and $(M/Z)/(m/z) = 3/6 = 1/2$ for the products Au_9^{1+} and Au_3^{1+}, respectively. Note, that for $\phi_z = \pi/2$ and $\phi_z = 3\pi/2$ the ion is at a turning point of its oscillatory motion. Therefore the amplitude will not change, i.e. $Z_{\max} = z_{\max}$. For $\phi_z = 0$ and $\phi_z = \pi$ the amplitude's change is maximal, since at these times the ion crosses the trap's center (see Fig. 7b).

With respect to the ion's energy the situation may be just the opposite from that of the change of amplitude: Consider the case of a change in charge state with no change in mass, for example, electron emission of dianions as discussed above. At the turning points (where the amplitude stays the same) the potential energy change due to the electric trapping field is maximal. In contrast, the total energy stays the same if the ion decays while crossing the trap's center; in this moment all the energy is concentrated in the kinetic energy contribution, which is almost unchanged by the electron loss.

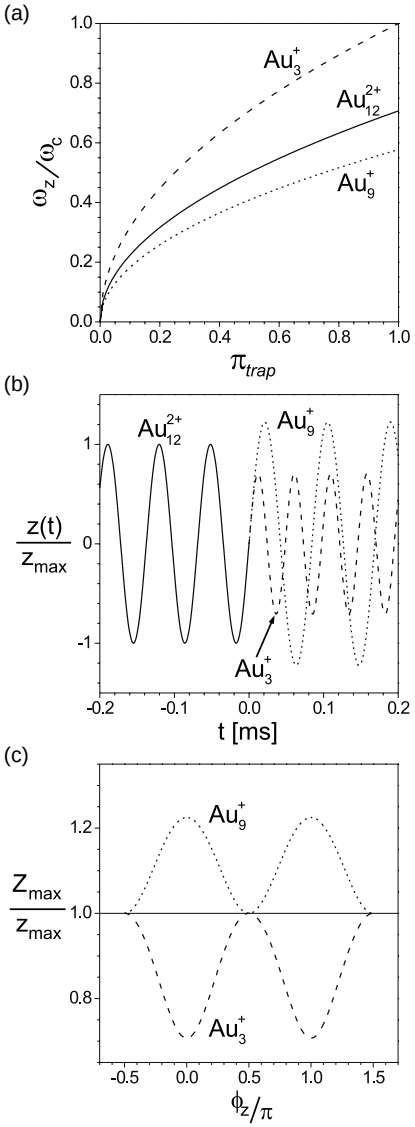

Fig. 7. (a) Axial frequency of Au_{12}^{2+} (solid line), Au_3^{1+} (dashed line) and Au_9^{1+} (dotted line) as a function of the trapping parameter π_{trap}. (b) Change of the axial motion after fission of Au_{12}^{2+} (solid line) into Au_3^{1+} (dashed line) and Au_9^{1+} (dotted line) at $t = 0$ with phase $\phi_z = 0$. (c) Amplitude of the axial motion $Z_{\max}$ of the fission products Au_3^{1+} (dashed line) and Au_9^{1+} (dotted line) relative to the initial amplitude $z_{\max}$ as a function of the phase ϕ_z.

3. Experimental procedure and results

The influence of a sudden change of the mass-over-charge ratio m/z on the ion motion will be demonstrated by a particular example: the electron emission from a dianionic metal cluster after collisional activation. The experimental setup is described in [29] and references therein: Singly charged metal clusters are produced in a pulsed laser vaporization source, transferred to a Penning trap and captured in flight. In the trap the stored ions may be subjected to a variety of interactions, for example, m/z-selective rf-excitations, photoexcitation, collisions or reactions with gas atoms or molecules,

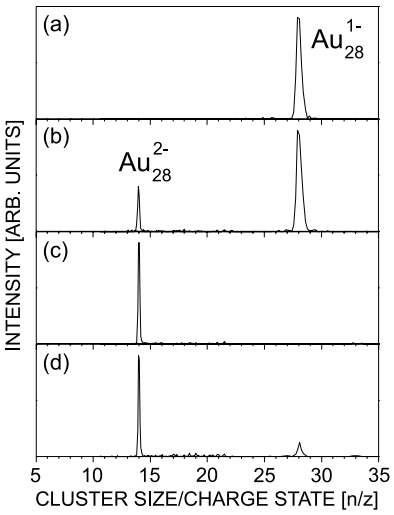

Fig. 8. TOF spectra (a) of size selected gold cluster ions Au_{28}^{1-}, (b) after application of an electron bath, (c) of charge selected dianions Au_{28}^{2-}, and (d) after photoexcitation (from [24]).

and collisions with electrons from an external electron gun. The reaction product ions as well as the remaining precursor ions are finally ejected into a time-of-flight mass spectrometer for single-ion-counting mass analysis.

In the case of metal cluster dianions, size-selected singly charged clusters are bathed in a sea of electrons that are stored simultaneously in the ion trap and eventually attach to the monoanions [22,30]. These low energy electrons are produced by ionization of argon gas that is pulsed into the trap volume. After a reaction time of one second the remaining singly charged clusters are removed from the trap by dipolar rf-excitation of the corresponding cyclotron motion. The size and charge-state selected dianions are thus prepared to be investigated by, for example, photoexcitation or collisional activation.

The production sequence is shown in Fig. 8 in form of TOF-spectra that are taken after (a) size-selection of a monoanion Au_{28}^{2-}, (b) reaction with an electron bath in the trap for one second, i.e. production of dianions Au_{28}^{2-}, (c) removal of the monoanions by dipolar excitation, and (d) irradiation with a Nd:YAG laser pulse at $\lambda = 355\,\text{nm}$. In the given example about 7% of the dianions decayed by single electron emission and monoanions reappeared in the mass spectrum.

In case of collisional activation the energy that is needed for the decay process is incorporated by transforming kinetic energy of the ion into internal energy by multiple collisions with inert gas, for example, argon atoms. To this effect, the radius of the ions' cyclotron motion is increased by dipolar rf-excitation at a fixed frequency $\nu_+ = \omega_+/2\pi$. The ions acquire a cyclotron radius of [31]:

$$r_+ = \frac{E_\text{D} T_\text{D}}{2B} \tag{42}$$

where E_D is the amplitude of the dipolar rf-field and T_D the duration of the excitation. In this work $T_\text{D} = 1\,\text{ms}$ and

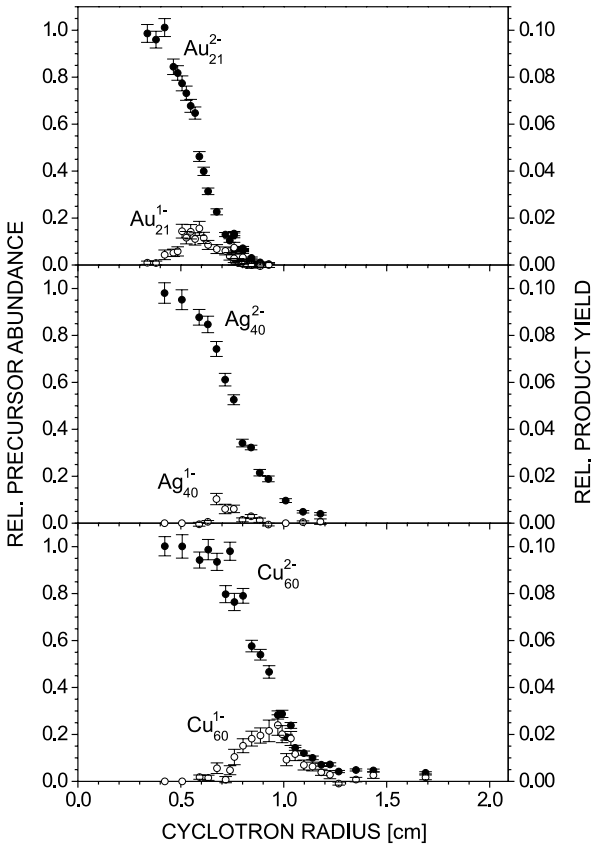

Fig. 9. Collisional activation of dianions Au_{21}^{2-} (top), Ag_{40}^{2-} (middle), and Cu_{60}^{2-} (bottom). The ion yield of the remaining precursor (full symbols) and product cluster anions (open symbols, note expanded scale) is plotted relative to a reference measurement (which is performed alternately without excitation) as a function of the cyclotron radius that is reached after dipolar excitation of the dianions.

$B = 5\,\text{T}$. The radius of the ring electrode, $r_0 = 20\,\text{mm}$, is an upper limit for the possible values of r_+. In order to minimize the initial amplitude of the ion motion prior to the excitation, the ions are centered in the middle of the trap by application of the buffer gas cooling method [32,33]. In addition, the electrons from the electron bath are removed from the trap to avoid a distortion of the electrostatic trapping potential and thus a shift of the motional frequencies due to the space charge [34]. The electron removal is accomplished by lowering the potential of an endcap electrode for $\Delta t = 1\,\mu\text{s}$ (suspended trapping [35]): The electrons leave the trap whereas the cluster anions, which are several orders of magnitude heavier, stay trapped.

For a systematic study the excitation amplitude E_D is varied. As an example Fig. 9 shows the relative abundance of metal cluster dianions of a similar mass-over-charge ratio m/z Au_{21}^{2-}, Ag_{40}^{2-}, and Cu_{60}^{2-} (full symbols) as a function of the cyclotron radius r_+ that is reached by dipolar excitation before the collision gas is pulsed into the trap. The open symbols denote the relative abundance of the product ions Au_{21}^{1-}, Ag_{40}^{1-}, and Cu_{60}^{1-}. Note, that the scale for the monoanions is expanded by a factor of 10 relative to the dianions.

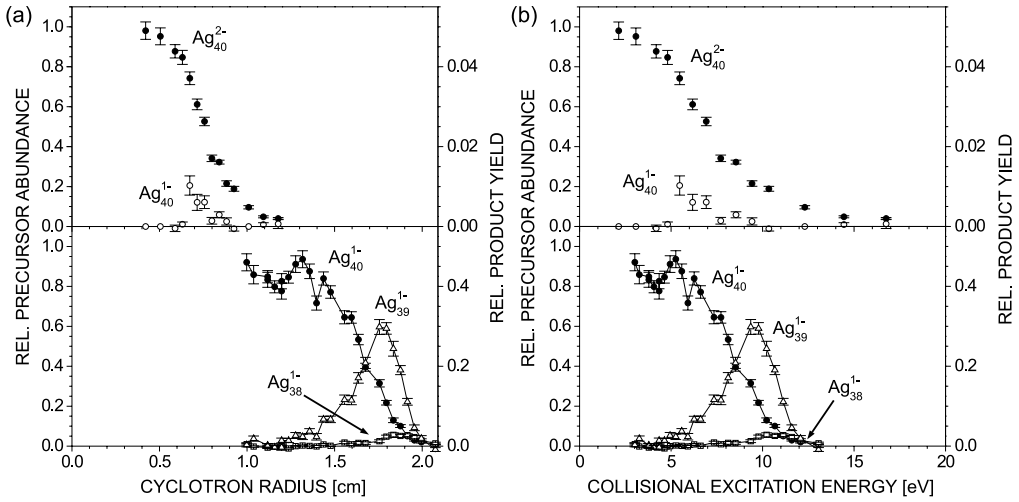

Fig. 10. Comparison of the collisional activation of Ag_{40}^{2-} (top) and Ag_{40}^{1-} (bottom) with the relative ion yields as a function of (a) the cyclotron radius after excitation, and (b) the collisional excitation energy. (Note the expanded scales of the product yields.)

For all three metals a decrease of the dianion yield is observed for radii larger than about 1/3 of the maximum radius r_0. The product anions, however, only reach a maximum value of the relative ion yield of about 1–3% and no further product anions, i.e. fragmentation products are observed. In Fig. 10 the result for the collisional activation of Ag_{40}^{2-} is compared to the result of collision-induced dissociation of the monoanionic precursor Ag_{40}^{1-}. Whereas no fragmentation product are observed in case of the excitation of dinaions Ag_{40}^{2-}, the excitation of the monoanions leads to fragmentation into Ag_{39}^{1-} and Ag_{38}^{1-}. The evaporation occurs at cyclotron radii close to the maximum radius $r_0 = 2.0$ cm, i.e. at radii, where no dianion signal is observed.

4. Discussion

At first glance the low number of product monoanions after collisional activation of the metal cluster dianions may be interpreted as a sequential emission of electrons. Since neutral particles cannot be stored in the ion trap, they are not observed at the detector. Some electron emission has been reported for singly charged silver cluster anions [36], but nevertheless a significant number of monoanionic product clusters should be observed after electron emission from the dianionic precursor clusters. The collisional activation of singly charged metal clusters, as for example, in case of Ag_{40}^{1-}, shows monomer evaporation as the dominant decay process (see Fig. 10).

The results are further emphasized by investigating the relative ion yield as a function of the collisional excitation energy. The kinetic energy of the anions after dipolar excitation is given by:

$$E_{\mathrm{kin},+} = \frac{1}{2} m\omega_+^2 r_+^2 \approx \frac{1}{8}\frac{q^2 E_{\mathrm{D}}^2 T_{\mathrm{D}}^2}{m} \tag{43}$$

which is transformed into the collisional excitation energy:

$$E_{\mathrm{coll}} \approx C_{\mathrm{mat}} \frac{m_{\mathrm{Ar}}}{m_{\mathrm{Ar}} + m_{\mathrm{atom}}} E_{\mathrm{kin},+} + E_{\mathrm{th}} \tag{44}$$

by use of the impulsive (multi-)collision theory [37,38]. An empirical correction factor $C_{\mathrm{mat}} = 0.4$ is applied to account for the actual energy transfer in each collision [39] and E_{th} is the thermal energy of the cluster prior to the collision where room temperature is assumed. In Fig. 10b the relative abundance of Ag_{40}^{2-}, Ag_{40}^{1-} and their products after collisional activation is plotted as a function of the collisional excitation energy. (Note, that the scale for the products is expanded by a factor of 20 and 2, respectively.) The intensity of clusters of both charge states decreases within a similar energy range. In case of the dianions Ag_{40}^{2-}, the first product, Ag_{40}^{1-}, should decay via fragmentation and not electron emission and thus at higher energies if not Ag_{40}^{1-} then Ag_{39}^{1-} should appear in the mass spectrum. Obviously, the change of the ion motion due to the drastic change in m/z, i.e. $M/Z = 2m/z$, leads to the loss of the cluster ions from the trap.

From the description of the ion motion given above (see Section 2), a maximum radius of $r_+ \simeq 0.62$ cm for Au_{21}^{2-}, $r_+ \simeq 0.61$ cm for Ag_{40}^{2-} and $r_+ \simeq 0.62$ cm for Cu_{60}^{2-} is derived for the moment of electron emission if ion loss is to be avoided, i.e. the new trajectory of the monoanionic products does not exceed the radial dimension of the ion trap. For the gold and silver cluster dianions the decrease of the monoanionic clusters is described well within these assumptions. For the copper cluster dianions the relative product yield seems to decrease at larger initial cyclotron radii (see Fig. 9). Note however, that the calculated r_+ values are only very rough estimates. In particular, the decrease of the cyclotron radius after rf excitation due to the collisions (which are by nature a necessary component of the collisional activation) is not taken into account. Since Cu_{60} has a higher number of internal degrees of freedom than Ag_{40} and Au_{21}, a higher excita-

Table 1
Resulting radial and axial amplitudes of ion motion, $R_+ + R_-$ and Z_{max}, as compared to the initial amplitudes, r_+, r_-, and z_{max}, after unimolecular process which change the mass-over-charge ratio from m/z to M/Z as discussed in Section 2

Before	After m/z-change	
	$M/Z > m/z$	$M/Z < m/z$
Cyclotron only ($r_- = 0$)	$R_+ + R_- > r_+$	$R_+ + R_- = r_+$
Magnetron only ($r_+ = 0$)	$R_+ + R_- > r_-$	$R_+ + R_- = r_-$
Axial (z_{max})	$Z_{max} > z_{max}$	$Z_{max} < z_{max}$

tion energy, i.e. a larger cyclotron radius, is expected before (thermionic) electron emission sets in. This may explain the observation of the copper clusters at a slightly higher cyclotron excitation where the gold and silver cluster signals have already disappeared.

5. Summary and outlook

In general the sudden change of the mass-over-charge ratio m/z leads to changes of the amplitudes of the ion motion in a Penning trap. This may increase the extension of the trajectory as summarized in Table 1 and may lead to ion loss from the trap. Especially experiments that employ an ICR trap for collision-induced dissociation (or collisional activation) of molecules have to be examined with respect to the decay channels and the resulting changes of the ion motion. In case of electron emission of dianionic metal clusters it has been shown, that the change of m/z results in a significant loss of product ions. Similar effects are expected for investigations of the fission of multiply charged clusters [27,28] and the decay of multiply protonated biomolecules.

By use of laser excitation of the ions after centering in the trap an ion loss due to the effects discussed can be avoided. Thus, the forthcoming experiments on dianions at the Cluster Trap will concentrate on laser activation [24].

Acknowledgements

This work has been supported by the DFG and the EU network “CLUSTER COOLING”.

References

[1] A.G. Marshall, Acc. Chem. Res. 18 (1985) 316.
[2] A.G. Marshall, Int. J. Mass Spectrom. 200 (2000) 331.
[3] D. Wobschall, J.R. Graham Jr., D.P. Malone, Phys. Rev. 131 (1963) 1565.
[4] D. Wobschall, Rev. Sci. Instrum. 36 (1965) 466.
[5] R.T. McIver Jr., Rev. Sci. Instrum. 41 (1970) 555.
[6] L. Schweikhard, H.-J. Kluge (Eds.), Proceedings of the Euroconference: Atomic Physics at Accelerators (APAC 99): Laser Spectroscopy and Applications, Hyperfine Interact. 127 (2000).
[7] D. Lunney (Ed.), Proceedings of the Euroconference: Atomic Physics at Accelerators (APAC 2000): Atomic Mass Measurements, Hyperfine Interact. 132 (2001).
[8] J.U. Andersen (Ed.), Proceedings of the Euroconference: Atomic Physics at Accelerators (APAC 2001): Stored Particles and Fundamental Physics, Hyperfine Interact. 146/147 (2003).
[9] M.B. Comisarow, A.G. Marshall, Chem. Phys. Lett. 25 (1974) 282.
[10] J.W. Cooley, J.W. Tukey, Math. Comput. 19 (1965) 297.
[11] A.G. Marshall, F.R. Verdun, Fourier Transforms in NMR, Optical, and Mass Spectrometry: A User’s Handbook, Elsevier, Amsterdam, 1990.
[12] I.J. Amster, J. Mass Spectrom. 31 (1996) 1325.
[13] A.G. Marshall, C.L. Hendrickson, G.S. Jackson, Mass Spectrom. Rev. 17 (1998) 1.
[14] A.G. Marshall, C.L. Hendrickson, Int. J. Mass Spectrom. 215 (2002) 59.
[15] R.T. McIver, R.L. Hunter, W.D. Bowers, Int. J. Mass Spectrom. Ion Process. 64 (1985) 67.
[16] J.M. Alford, P.E. Williams, D.J. Trevor, R.E. Smalley, Int. J. Mass Spectrom. Ion Process. 72 (1986) 33.
[17] H. Schnatz, G. Bollen, P. Dabkiewicz, P. Egelhof, F. Kern, H. Kalinowsky, L. Schweikhard, H. Stolzenberg, H.-J. Kluge, Nucl. Intr. Methods A 251 (1986) 17.
[18] M. Karas, D. Bachmann, U. Bahr, F. Hillenkamp, Int. J. Mass Spectrom. Ion Process. 78 (1987) 53.
[19] K. Tanaka, H. Waki, Y. Ido, S. Akita, Y. Yoshida, T. Yoshida, Rapid Commun. Mass Spectrom. 2 (1988) 151.
[20] J.B. Fenn, M. Mann, C.K. Meng, S.F. Wong, C.M. Whitehouse, Science 246 (1989) 64.
[21] L. Schweikhard, J. Ziegler, H. Bopp, K. Lützenkirchen, Int. J. Mass Spectrom. Ion Process. 141 (1995) 77.
[22] A. Herlert, L. Schweikhard, Int. J. Mass Spectrom. 229 (2003) 19.
[23] A. Herlert, L. Schweikhard, M. Vogel, in: F. Anderegg, L. Schweikhard, C.F. Driscoll (Eds.), AIP Conference Proceedings on Non-Neutral Plasma Physics IV, vol. 606, 2002, p. 652.
[24] L. Schweikhard, K. Hansen, A. Herlert, M.D. Herráiz Lablanca, G. Marx, M. Vogel, Int. J. Mass Spectrom. 219 (2002) 363.
[25] L.S. Brown, G. Gabrielse, Rev. Mod. Phys. 65 (1986) 25.
[26] S. Guan, A.G. Marshall, Int. J. Mass Spectrom. Ion Process. 146/147 (1995) 261.
[27] J. Ziegler, G. Dietrich, S. Krückeberg, K. Lützenkirchen, L. Schweikhard, C. Walther, Hyperfine Interact. 115 (1998) 171.
[28] J. Ziegler, G. Dietrich, S. Krückeberg, K. Lützenkirchen, L. Schweikhard, C. Walther, Int. J. Mass Spectrom. 202 (2000) 47.
[29] L. Schweikhard, K. Hansen, A. Herlert, G. Marx, M. Vogel, Eur. Phys. J. D 24 (2003) 137.
[30] A. Herlert, S. Krückeberg, L. Schweikhard, M. Vogel, C. Walther, Phys. Scr. T80 (1999) 200.
[31] L. Schweikhard, A.G. Marshall, J. Am. Soc. Mass Spectrom. 4 (1993) 433.
[32] G. Savard, St. Becker, G. Bollen, H.-J. Kluge, R.B. Moore, L. Schweikhard, H. Stolzenberg, U. Wiess, Phys. Lett. A 158 (1991) 247.
[33] L. Schweikhard, S.H. Guan, A.G. Marshall, Int. J. Mass Spectrom. Ion Process. 120 (1992) 71.
[34] L. Schweikhard, A. Herlert, G. Marx, in: M. Schauer, T. Mitchell, R. Nebel (Eds.), AIP Conference Proceedings on Non-Neutral Plasma Physics V, vol. 692, 2003, p. 203.
[35] D.A. Laude, S.C. Beu, Anal. Chem. 61 (1989) 2422.
[36] Y. Shi, V.A. Spasov, K.M. Ervin, J. Chem. Phys. 111 (1999) 938.
[37] E. Uggerud, P.J. Derrick, J. Phys. Chem. 95 (1991) 1430.
[38] H.J. Cooper, P.J. Derrick, H.D.B. Jenkins, E. Uggerud, J. Phys. Chem. 97 (1993) 5443.
[39] S. Krückeberg, G. Dietrich, K. Lützenkirchen, L. Schweikhard, C. Walther, J. Ziegler, J. Chem. Phys. 110 (1999) 7216.